Microsc. Microanal. 14, 418–432, 2008
doi:10.1017/S1431927608080896

Microscopy AND Microanalysis

Analysis of Heterogeneous Mitochondria Distribution in Somatic Cell Nuclear Transfer Porcine Embryos

Zhisheng Zhong,[1] Yanhong Hao,[2] Rongfeng Li,[2] Lee Spate,[2] David Wax,[2] Qing-Yuan Sun,[3] Randall S. Prather,[2] and Heide Schatten[1,*]

[1]*Department of Veterinary Pathobiology, University of Missouri-Columbia, Columbia, MO 65211, USA*
[2]*Division of Animal Science, University of Missouri-Columbia, Columbia, MO 65211, USA*
[3]*State Key Laboratory of Reproductive Biology, Institute of Zoology, Chinese Academy of Sciences, Beijing 100080, P.R. China*

Abstract: We previously reported that translocation of mitochondria from the oocyte cortex to the perinuclear area indicates positive developmental potential that was reduced in porcine somatic cell nuclear transfer (SCNT) embryos compared to *in vitro*–fertilized (IVF) embryos (Katayama, M., Zhong, Z.-S., Lai, L., Sutovsky, P., Prather, R.S. & Schatten, H. (2006). *Dev Biol* **299**, 206–220.). The present study is focused on distribution of donor cell mitochondria in intraspecies (pig oocytes; pig fetal fibroblast cells) and interspecies (pig oocytes; mouse fibroblast cells) reconstructed embryos by using either pig fibroblasts with mitochondria-stained MitoTracker CMXRos or YFP-mitochondria 3T3 cells (pPhi-Yellow-mito) as donor cells. Transmission electron microscopy was employed for ultrastructural analysis of pig oocyte and donor cell mitochondria. Our results revealed donor cell mitochondrial clusters around the donor nucleus that gradually dispersed into the ooplasm at 3 h after SCNT. Donor-derived mitochondria distributed into daughter blastomeres equally (82.8%) or unequally (17.2%) at first cleavage. Mitochondrial morphology was clearly different between donor cells and oocytes in which various complex shapes and configurations were seen. These data indicate that (1) unequal donor cell mitochondria distribution is observed in 17.2% of embryos, which may negatively influence development; and (2) complex mitochondrial morphologies are observed in IVF and SCNT embryos, which may influence mitochondrial translocation and affect development.

Key words: somatic cell nuclear transfer (SCNT), mitochondrial heterogeneity, pleomorphic mitochondria, oocytes, pig cloning, development, mitochondrial ultrastructure

Introduction

Accurate distribution of mitochondria is critically important for embryo development to carry out vital spatiotemporal cellular functions including adenosine triphosphate (ATP) production, cellular oxidation, signal transduction, and calcium regulation. Asymmetrical and abnormal mitochondria distribution is associated with developmental abnormalities in *in vitro*–fertilized oocytes (Van Blerkom et al., 1995, 2000; reviewed in Schatten et al., 2005) that may be the result of imbalanced metabolism and ATP generating capacity in individual blastomeres.

In fertilized eggs, sperm mitochondria become destroyed within the ooplasm by oocyte-driven ubiquitination (Sutovsky et al., 1999, 2003; Sutovsky, 2004) allowing a homogeneous maternally inherited mitochondrial population, while in cloned embryos mitochondria from both the donor cell and the enucleated oocyte contribute to the reconstructed egg resulting in a heterogeneous mitochondrial population (Steinborn et al., 2000, 2002; Hiendleder et al., 2004; St. John et al., 2004; reviewed in Schatten et al., 2005; Takeda et al., 2006; Ferreira et al., 2007).

Our previous studies showed that accurate mitochondrial translocation from the oocyte cortex to the ooplasm and perinuclear area is indicative of positive developmental potential (Katayama et al., 2006). We also showed that mitochondrial translocation is reduced in somatic cell nuclear transfer (SCNT) embryos, but that a number of reconstructed oocytes showed perinuclear mitochondria aggregation around the donor cell nucleus that did not translate into positive developmental potential, suggesting the possibility that these perinuclear mitochondrial aggregates may be derived from donor cells and may not be the result of oocyte mitochondrial translocations. We considered the possibility that donor cell mitochondria may not be distributed accurately because distribution would be in an opposite direction compared to oocyte mitochondria that are translocated from the oocyte cortex to the perinuclear area. We considered that translocation incompatibilities along microtubules may play a role in accurate mitochondrial distribution.

Received June 4, 2008; accepted July 23, 2008
*Corresponding author. E-mail: SchattenH@missouri.edu

Different from fertilization, in cloned embryos mitochondria are translocated by microtubules that are nucleated and organized by the donor cell centrosome and not by microtubules of the sperm aster, as is the case in *in vitro* fertilization (IVF). In fertilized and SCNT eggs, microtubules need to elongate toward the oocyte cortex to translocate mitochondria into the ooplasm and perinuclear area.

There are several possible explanations to account for the reduced mitochondrial translocation in reconstructed eggs, which may include insufficient microtubule organization from the donor cell centrosome that normally nucleates shorter microtubules sufficient for the much smaller somatic cells, while in the ca. ten times larger oocyte cell, it is necessary to organize longer microtubules that are able to contact mitochondria at the egg cortex. Another explanation for reduced mitochondria translocation may be related to morphological differences between donor cell and oocyte mitochondria. Donor cell mitochondria are sausage-shaped and display well-organized cristae while oocyte mitochondria display multiple and complex morphologies with few to no cristae in the early embryo stages (Krause et al., 1992). Differences in surface components between the two different mitochondrial populations and the complex oocyte mitochondrial morphologies may play a role in reduced translocation to the perinuclear area in porcine SCNT eggs.

In the present study we focused on (1) distribution of donor cell mitochondria and (2) ultrastructure of mitochondria in reconstructed pig oocytes. We investigated the distribution of donor cell mitochondria in interspecies reconstructed pig embryos by using mouse 3T3 fibroblast cells with mitochondria containing a yellow fluorescence protein (YFP) signal and enucleated pig oocytes in which mitochondria were stained with MitoTracker CMXRos to distinguish the two different mitochondrial populations and clearly follow their distribution and fate. We further used pig fibroblast cells and enucleated pig oocytes to study mitochondrial distribution in intraspecies reconstructed pig embryos. We show that donor cell mitochondria incorporate into the reconstructed embryo's mitochondrial pool. They remain tightly aggregated around the donor cell nucleus for ca. 30 min and disperse either equally (82.8%) or unequally (17.2%) into the two blastomeres after oocyte division.

Material and Methods

Cell Culture

Mouse 3T3 fibroblast-mitochondria-PhiYellow cells were obtained from Marinpharm (Berlin, Germany). A PhiYFP vector was transfected into 3T3 cells and a stable and strong mitochondria yellow fluorescence cell line was selected, which allows detailed investigation of mitochondrial dynamics within live and fixed cells. Cells were cultured as monolayer in DULBECCO'S MEM supplemented with 3.7 g/L $NaHCO_3$, 1.0 g/L D-glucose, 2 mM glutamine, 1% nonessential amino acids, 10% fetal calf serum, and 500 mg/L G418 antibiotics. Cells were subcultured one to two times per week.

Preparation, Maturation, and IVF of Pig Oocytes

Preparation

Porcine ovaries were obtained from a local slaughterhouse and transported to the laboratory at ca. 34°C. Follicular fluid from 3–6 mm antral follicles was aspirated with an 18-gauge syringe. Cumulus–oocyte complexes (COCs) with uniform cytoplasm and several layers of cumulus cells were selected and rinsed three times in TL-HEPES washing medium (TCM-199 medium was supplemented with 0.1% PVA, 3.05 mM D-glucose, 0.91 mM sodium pyruvate, 100 IU penicillin, 50 μg/ml streptomycin, 0.57 mM cysteine, and 10 ng/ml EGF).

Maturation

About 50–70 COCs per well were cultured in multidish plates containing TL-HEPES culture medium (TL-HEPES washing medium supplemented with 10 IU FSH, 10 IUml LH), covered with mineral oil. Oocytes were matured for 42–44 h at 39°C, 5% CO_2 in air (Abeydeera et al., 1998; Li et al., 2006).

In Vitro Fertilization

IVF was carried out as previously described with only minor modifications (Han et al., 1999*a*, 1999*b*). Oocytes were inseminated in a 100-μl drop of modified Tris-buffered medium (mTBM) containing 0.2% BSA (W/V) and 2 mM caffeine with frozen-thawed spermatozoa (5×10^5 cells/ml). Oocytes were removed from the fertilization drop at 4 to 5 h after insemination and cultured up to 7 days in 500-μl PZM-3 medium (Petters & Wells, 1993; Lai et al., 2002; Katayama et al., 2006; Li et al., 2006) containing 4 mg/ml BSA. Mitochondrial distribution, microtubules, and centrosomes were assessed during fertilization, cell division, and development (Sun et al., 2001). About 30 fertilized oocytes per group were collected at various time points postinsemination as indicated in the text. Key time points for development from fertilization to the blastocyst stages are 0 time, 4–6 h (sperm incorporation and sperm aster formation), 6–10 h (male pronuclear formation, enlargement of the sperm aster), 18–22 h (pronuclear apposition and radial aster formation), 24–28 h (mitotic metaphase formation), 24–32 h (cleavage and microtubule formation in the daughter cells), 44–52 h (4-cell stage), and 5–7 days (blastocyst formation).

Production of Nuclear Transfer Embryos

Cumulus–oocyte complexes matured for 42–44 h were vortexed for 4 min in 0.1% hyaluronidase (in TL-Hepes supplemented with 0.1% PVA) to remove cumulus cells. Cumulus cell-free (denuded) oocytes were transferred into a 50-μl

drop of manipulation medium (25 mM HEPES buffered TCM199 with 3 mg/mL BSA and 7.5 μg/mL cytochalasin B). Ooytes were enucleated with a 16–18 μm inner diameter injection pipette for aspiration of the first polar body and adjacent cytoplasm, where the MII spindle was located. One single donor cell was injected directly into the perivitelline space of each denuded oocyte. Fusion and activation of enucleated oocyte-donor cell reconstructions were accomplished by applying 2 DC pulses (1.2 kV/cm for 30 μs; 2 pulses separated by a 1-s interval) with a BTX Elector-Cell Manipulator 200 (BTX, San Diego, CA) in fusion medium (0.3 M mannitol, 0.1 mM $CaCl_2$, 0.1 mM $MgCl_2$, and 0.5 mM HEPES). Key time points from nuclear transfer to the blastocyst stages are 0 time, 1–3 h (beginning of decondensation of the transferred nucleus), 3–6 h (enlargement of the transferred nucleus), 22–24 h (cleavage and microtubule formation in the daughter cells), 44–48 h (4-cell stage), and 5–7 days (blastocyst formation).

Fluorescence and Immunofluorescence Microscopy

Fluorescence Microscopy of Mitochondria

MitoTracker® Orange CMXRos (Cat#: M7510, Molecular Probes, Inc. Eugene, OR) was diluted into 1 mM stock solution (in dimethyl sulfoxide, DMSO, Sigma). Live cells, oocytes, or embryos were stained with 1 μM CMXRos in culture medium for 30 min, and then washed three times. Samples were fixed with 4% paraformaldehyde for 10 min (somatic cells) or 45 min (oocytes/embryos). Following washes in PBS, samples were mounted in Vectashield mounting medium containing 4′, 6-diamidino-2-phenylindole (DAPI) to visualize DNA (H-1200, Vector Laboratories, Inc., Burlingame, CA) and analyzed with epi-fluorescence microscopy using a Zeiss Axiophot equipped with appropriate filters. Data were saved to a disk and subsequently processed by using Photoshop software. At least 30 samples in each group were analyzed in three repeated experiments.

Immunofluorescence Microscopy of Microtubules and Centrosomes

For immunofluorescence microscopy of microtubules and centrosomes, we used antibodies to α-tubulin (1:50; Sigma, Cat # F2168) to stain microtubules and γ-tubulin (1:300; Sigma, Cat# T5192) to detect centrosomes. For optimal staining, the zona pellucida of oocytes and embryos was removed by 0.25% pronase, washed in PBS, and then fixed in 4% (W/V) paraformaldehyde in PBS for 45 min at room temperature. Oocytes and embryos were washed three times in PBS, followed by permeabilization and lipid droplet extraction in 50% methanol (5 min), 100% methanol (5 min), and 100% acetone (5 min). Lipid extracted oocytes and embryos were rehydrated in 1% BSA PBS for 2 days. After blocking with 3% BSA for 1 h, samples were stained with the primary antibodies, washed three times, stained with 1:100 antirabbit IgG second antibodies (F1263, Sigma), and counterstained with 1 μg ml–1 DAPI in Vectashield mounting medium (Vector Laboratories, Burlingame, CA) to stain DNA. Oocytes/embryos were finally mounted on glass slides. All samples were observed with a Zeiss Axiophot. Images were processed with Photoshop software. At least 30 samples in each group were analyzed in three repeated experiments (Zhong et al., 2005).

Transmission Electron Microscopy

For ultrastructural studies, oocytes and embryos were fixed for 1 h in 2% glutaraldehyde in 0.1 M PBS buffer, pH 7.4, with 0.05% saponin and 0.2% tannic acid at various time points as described for immunofluorescence microscopy. Oocytes/embryos were washed three times and centrifuged at 800 g for 5 min. The supernatant was gently aspirated without disturbing the pellet. Two percent agar warmed to 50°C was gently added on top of the pellet and centrifuged to keep the pellet compact. After cooling of the pellet-containing agar, the pellet and a small volume of agar surrounding the pellet were cut out and stored in PBS. Oocytes/embryos were then postfixed in 1% OsO_4 for 60 min after rinses with 0.1 M PBS (Schatten et al., 2000*a*, 2000*b*; Schatten & Ris, 2002, 2004). After dehydrations samples were embedded in Epon resin (Schatten & Ris, 2002, 2004). Thin-sectioned uranyl-acetate and lead citrate-stained cells were analyzed with a Philips CM120 scanning transmission electron microscope instrument.

Results

Mitochondria display significant morphological differences in embryo cells compared to somatic cells and within oocytes there are significant variations in mitochondrial shapes and forms. We used transmission electron microscopy (TEM) and fluorescence microscopy to analyze how mitochondria distribute into blastomeres of reconstructed (SCNT) embryos that contain a heterogeneous mitochondrial population compared to IVF oocytes that contain a maternally-inherited homogeneous mitochondrial population. To analyze whether there are differences in intraspecies and interspecies mitochondrial distribution, we used Mitotracker staining for donor cell and oocyte mitochondria in intraspecies (pig oocytes; pig fetal fibroblast cells) experiments and mouse 3T3 fibroblast-mitochondria-PhiYellow donor cells to trace the fate of mitochondria in interspecies pig-mouse (pig oocytes; mouse fibroblast cells) reconstructed eggs.

Fluorescence and Immunofluorescence Microscopy

Donor Cells

The mitochondrial distribution patterns in fibroblast cells are shown in Fig. 1. Figure 1A is a representative cell from the YFP-mitochondria cell culture displaying bright yellow/

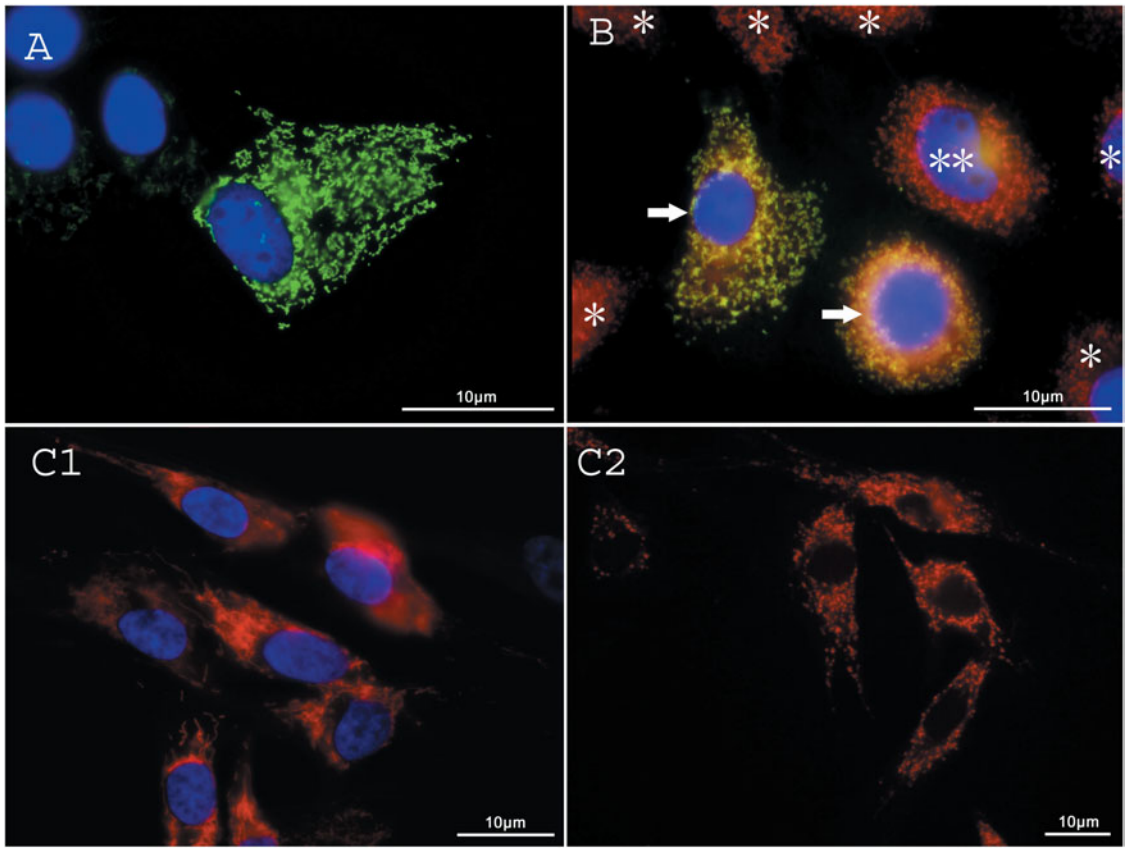

Figure 1. YFP-mitochondria 3T3 cells and pig fibroblast cells stained with Mitotracker CMXRos. **A:** YFP-mitochondria 3T3 cells with bright yellow-green fluorescence. **B:** YFP-mitochondria 3T3 cells stained with Mitotracker CMXRos. YFP expression varies in YFP-mitochondria 3T3 cells: cells with high expression are identified by arrow, cells with low expression are identified by *, and cells with intermediate expression are identified by **. **C1**, **C2:** Pig fibroblast cells stained with Mitotracker CMXRos: blue, DNA; green, YFP-mitochondria; red, mitochondria stained with CMXRos.

green fluorescence. The YFP-mitochondria fluorescence pattern matches that of cells stained with CMXRos as shown in Fig. 1B of a cell with YFP and CMXRos signals. In Figures 1C1 and 1C2, typical mitochondrial staining patterns with CMXRos are seen in pig fetal fibroblast cells. Most of the mitochondria either in YFP-mitochondria 3T3 cells or in fetal pig fibroblast cells display elongated shapes that are characteristic for somatic cell mitochondria.

IVF Embryos

Mature pig oocytes (MII stage oocytes), IVF embryos, and blastocysts (day 6) were double stained with CMXRos and anti-α-tubulin antibody to evaluate mitochondria and microtubule distribution. Figure 2A shows mitochondria (red) evenly distributed throughout the ooplasm and around the MII spindle (green) area, which is different from that reported for mouse MII oocytes in which mitochondria are clustered around the MII oocyte spindle (Calarco, 1995). In pigs, the MII spindle is oriented perpendicular to the oocyte cortex. Figures 2B and 2C show IVF 2-cell stage blastomeres at 28 h after insemination with microtubule arrays around the pronuclei and cytoplasmic mitochondrial distribution. Cytoplasmic mitochondrial distribution is also seen in 4-cell stage IVF blastomeres at 50 h after insemination (Fig. 2D,E). A day 6 blastocyst double stained with CMXRos and anti-α-tubulin antibody is seen in Figure 2F with mostly interphase cells displaying even cytoplasmic mitochondrial distribution and one mitotic cell displaying a prominent mitotic spindle labeled with anti-α-tubulin antibody.

Nuclear Transfer Embryos

To trace the fate of donor cell-derived mitochondria in intraspecies cloned embryos, fetal pig fibroblasts were preloaded with CMXRos before embryo reconstruction. At 30 min after fusion, the donor cell-derived mitochondria in reconstructed embryos were located near the donor cell nucleus (Fig. 3A) and dispersed into the ooplasm by 6 h of culture (Fig. 3B). The donor cell centrosome is detected with γ-tubulin as

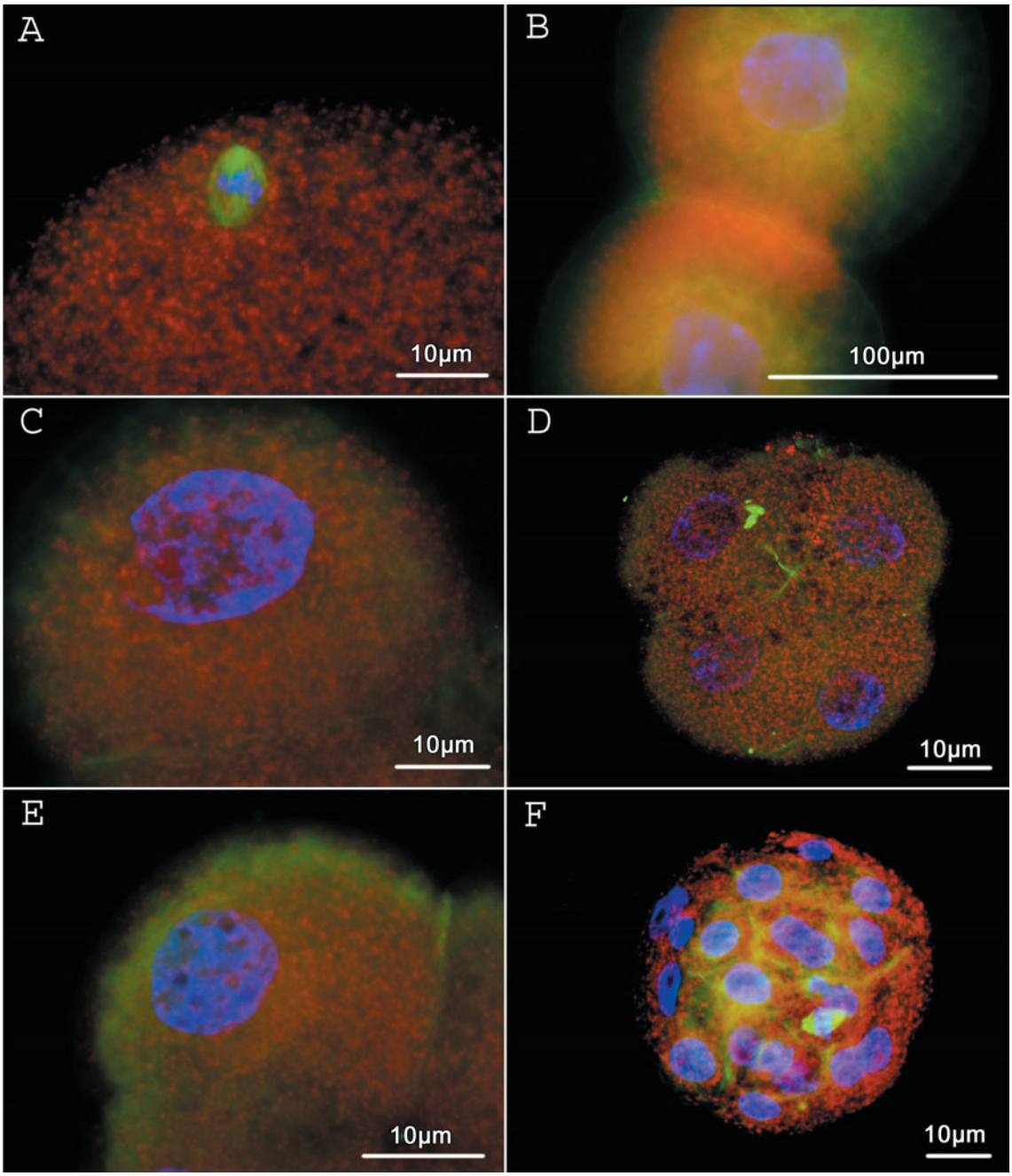

Figure 2. A: MII pig oocyte double stained with CMXRos and anti-tubulin antibody. **B**,**C**: IVF 28 h, 2-cell stage blastomeres. **D**,**E**: IVF 50 h, 4-cell stage blastomeres. **F**: IVF day 6 blastocyst. Blue, DNA; green, microtubules; red, mitochondria.

shown in Fig. 3C at 1.5 h after NT. At 30 and 66 h after fusion, the donor cell-derived mitochondria dispersed into daughter blastomeres during cleavage (Fig. 3D,E), which is a pattern seen throughout development and shown in Fig. 3F at day 7 after reconstruction.

To determine the fate of donor cell mitochondria in interspecies SCNT embryos, we next used YFP-mitochondria 3T3 cells as donor cells and enucleated CMXRos preloaded MII stage pig oocytes as recipients. Donor cell derived-mitochondria were detected clearly around the donor cell nucleus at 1.5 h after NT (Fig. 4A); dispersion was observed at 3 h after NT (Fig. 4B); it was more difficult to detect mitochondria after 12 h of fusion, which may indicate dispersion beyond detection by fluorescence microscopy; it also leaves the possibility that they might be recognized as foreign and become destroyed within the recipient ooplasm.

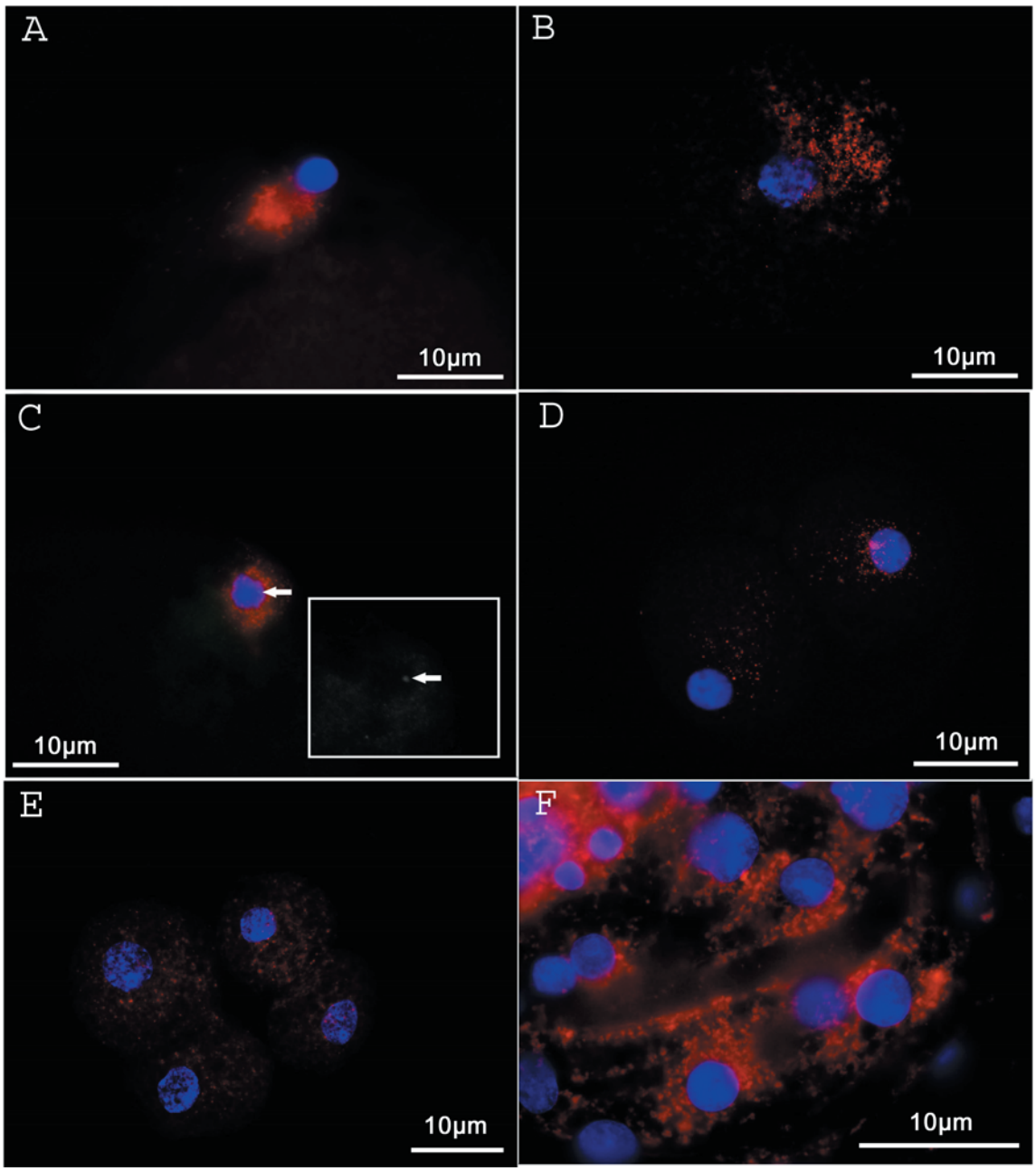

Figure 3. **A:** Donor cell preloaded with CMXRos, 30 min after fusion. Donor-derived mitochondria locate near the donor nucleus. **B:** Donor cell proloaded with CMXRos, 6 h after fusion. Donor-derived mitochondria are dispersed into the ooplasm. **C:** Donor cell preloaded with CMXRos, 1.5 h after fusion, stained with gamma-tubulin antibody (green); insert image: gamma-tubulin (gray). **D**, **E:** Donor cells proloaded with CMXRos, (**D**) 30 h and (**E**) 66 h after fusion. Donor-derived mitochondria distributed into two or four daughter blastomeres. **F:** NT day 7 embryo, stained with Mitotracker CMXRos. Blue, DNA; red, mitochondria.

Because pig oocytes are rich in lipid droplets, we considered that mitochondria detection might be obscured by the abundant lipid droplets; we prepared SCNT recipient embryos from which the lipid droplets had been removed to better observe donor-derived mitochondria. After lipid removal, the dark enucleated MII pig oocytes became transparent (data not shown). In intraspecies SCNT embryos, donor-derived mitochondria could be detected for at least 2 days (Fig. 5A–D). We could more clearly see donor-derived mitochondria that had distributed into each of the daughter blastomeres displaying variations in distribution patterns. Equal mitochondrial distribution (82.8%, 24/29;

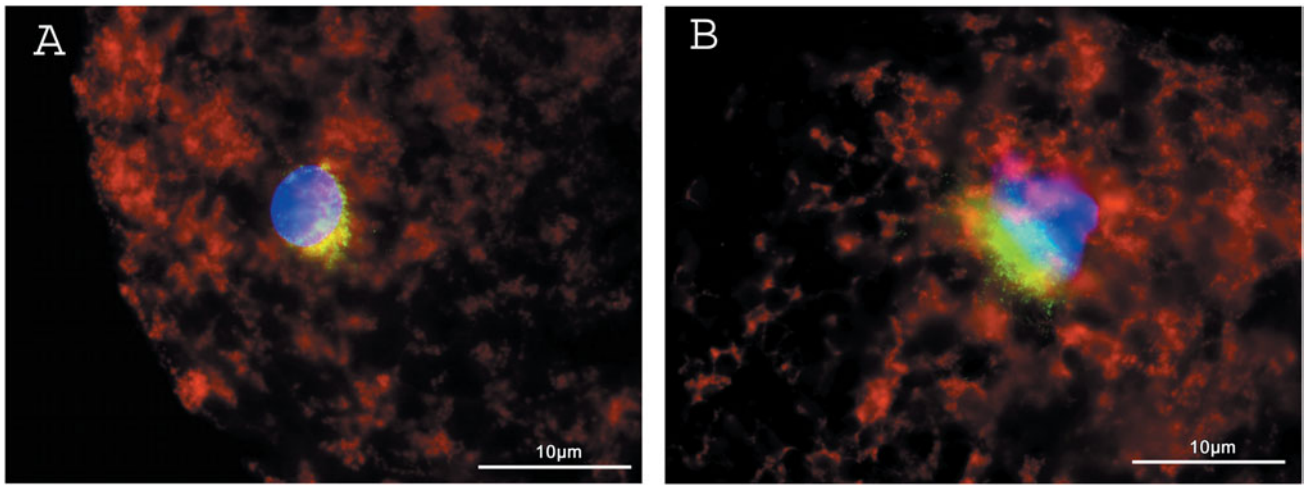

Figure 4. YFP-mitochondria 3T3 cells as donor cells, CMXRos preloaded MII pig oocytes as recipients; NT embryo (**A**) 1.5 h and (**B**) 3 h after fusion. Donor-derived mitochondria are dispersed into the ooplasm. Blue, DNA; green, donor-derived YFP mitochondria; red, oocyte-derived recipient mitochondria.

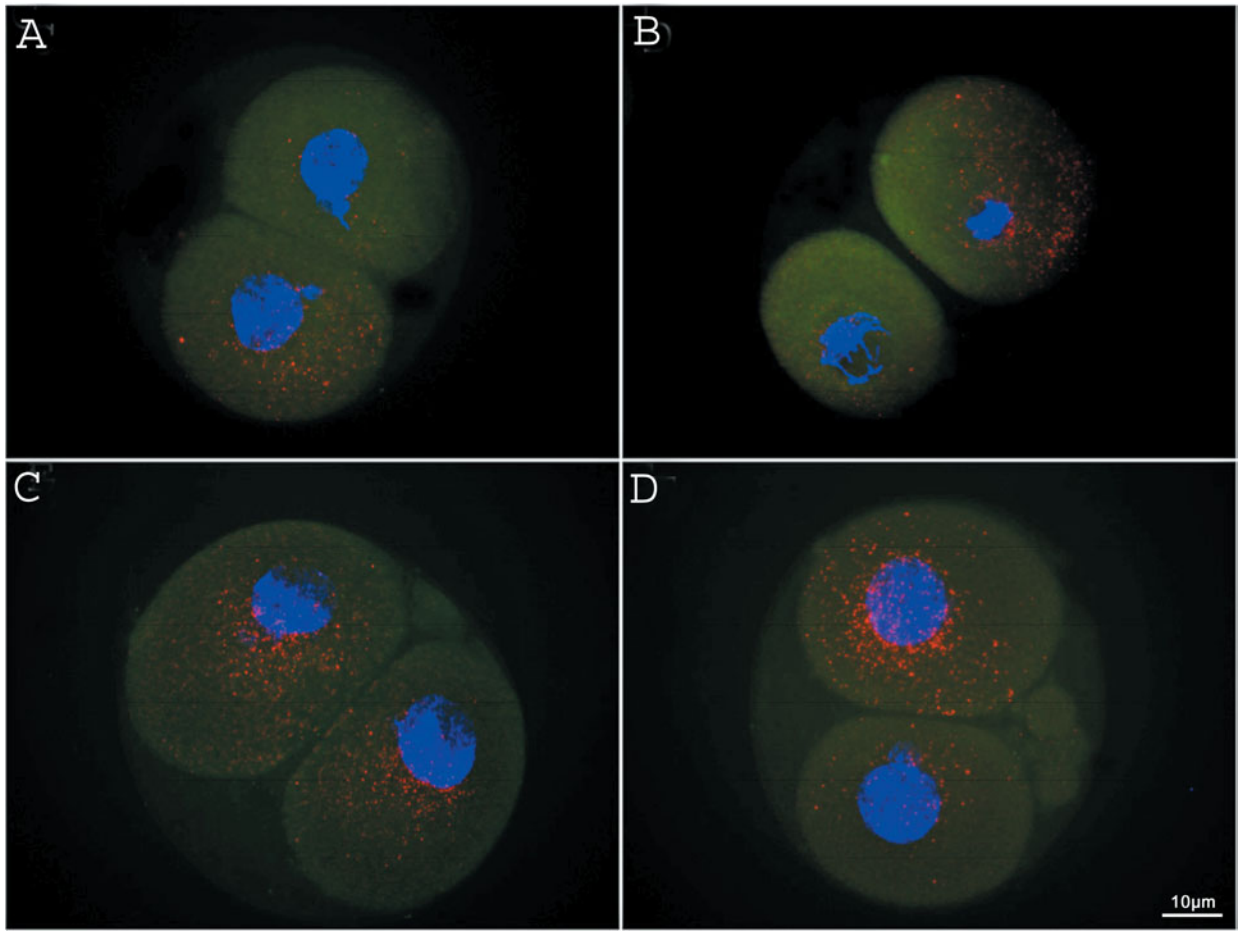

Figure 5. A–D: CMXRos preloaded fibroblast cells as donor cells, lipid droplet-removed pig oocytes as recipients; NT embryos cultured for 30 h after fusion. Donor-derived mitochondria in two daughter cells display variable distribution. **A**, **B**, **D:** Donor-derived mitochondria distribution in two daughter cells is unequal. Peri-pronuclear aggregation is seen in **C** and **D**. Blue, DNA; red, donor-derived CMXRos preloaded mitochondria.

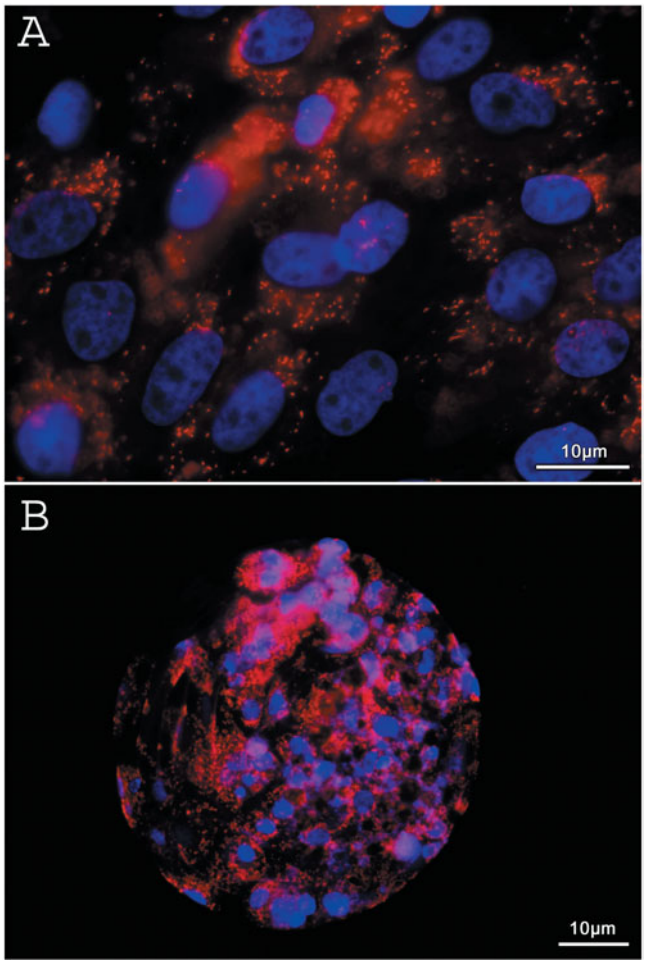

Figure 6. A: Pig fetal fibroblast cells preloaded with CMXRos, cultured for 4 days. **B:** CMXRos preloaded oocytes, then fertilized and cultured to day 8. Blue, DNA; red, mitochondria.

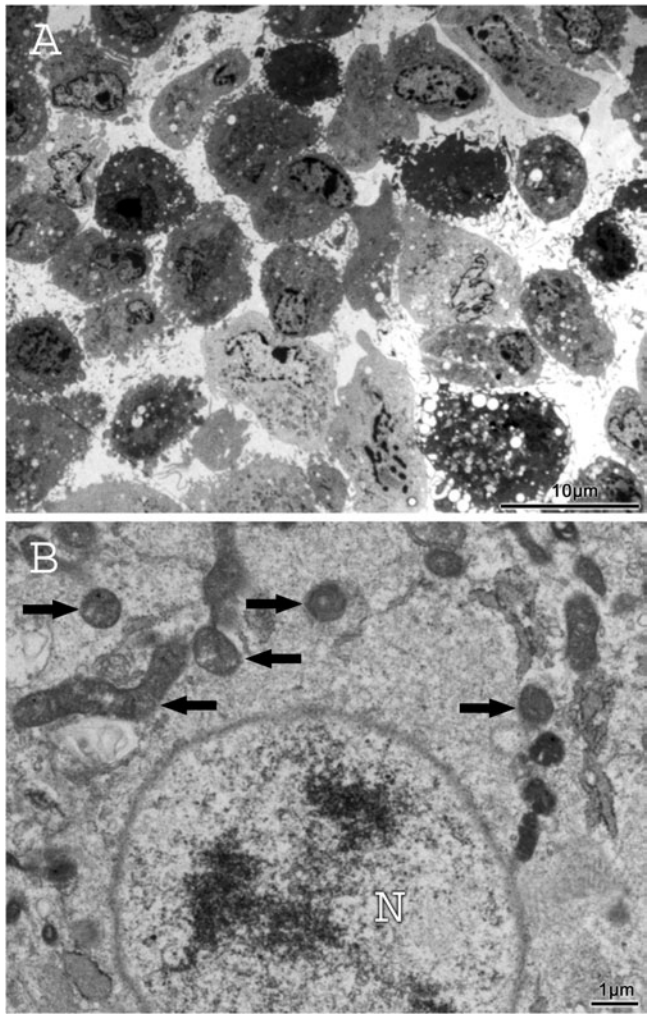

Figure 7. A: TEM—low magnification TEM shows porcine fetal fibroblast cells synchronized by serum starvation. **B:** TEM of selected area of porcine fetal fibroblast cell with typical somatic cell mitochondria (arrows) around the nucleus (N).

as seen in Fig. 5C) and unequal mitochondrial distribution (17.2%, 5/29; as seen in Fig. 5A,B,D) were observed for donor cell-derived mitochondria. Figure 5C,D displays more clearly perinuclear mitochondrial distribution (44.8%; 13/29). Similar results of perinuclear mitochondrial distribution were obtained when YFP-mitochondria 3T3 cells were used as donor cells and MII pig oocytes as recipients (data not shown).

We also examined whether CMXRos might have a negative long-term effect on cell and embryo development and determined that no obvious harmful effect on embryo development was seen after 4 days (Fig. 6A) and 8 days (Fig. 6B) of live CMXRos stained embryo cultures as judged by the normal morphology of blastocysts displaying still clear CMXRos mitochondrial staining.

Transmission Electron Microscopy

Because mitochondria display significantly different morphologies in embryo cells compared to somatic cells, we investigated on an ultrastructural level whether there might be differences in how oocyte mitochondria distribute in NT cells that contain a heterogeneous mitochondrial population compared to IVF oocytes that contain a maternally-inherited homogeneous mitochondrial population. We further focused on ultrastructural features of oocyte mitochondria to determine potential differences in morphology and distribution in IVF and NT oocytes. All images shown here are representative for the specific time points.

Fetal Fibroblast Cells before Nuclear Transfer

A low magnification TEM image of fetal fibroblast cells is shown in Fig. 7A in which various cellular and nuclear morphologies are apparent. The higher magnification image in Fig. 7B shows a selected area around the nucleus (N) displaying typical elongated (sausage-shaped) somatic cell

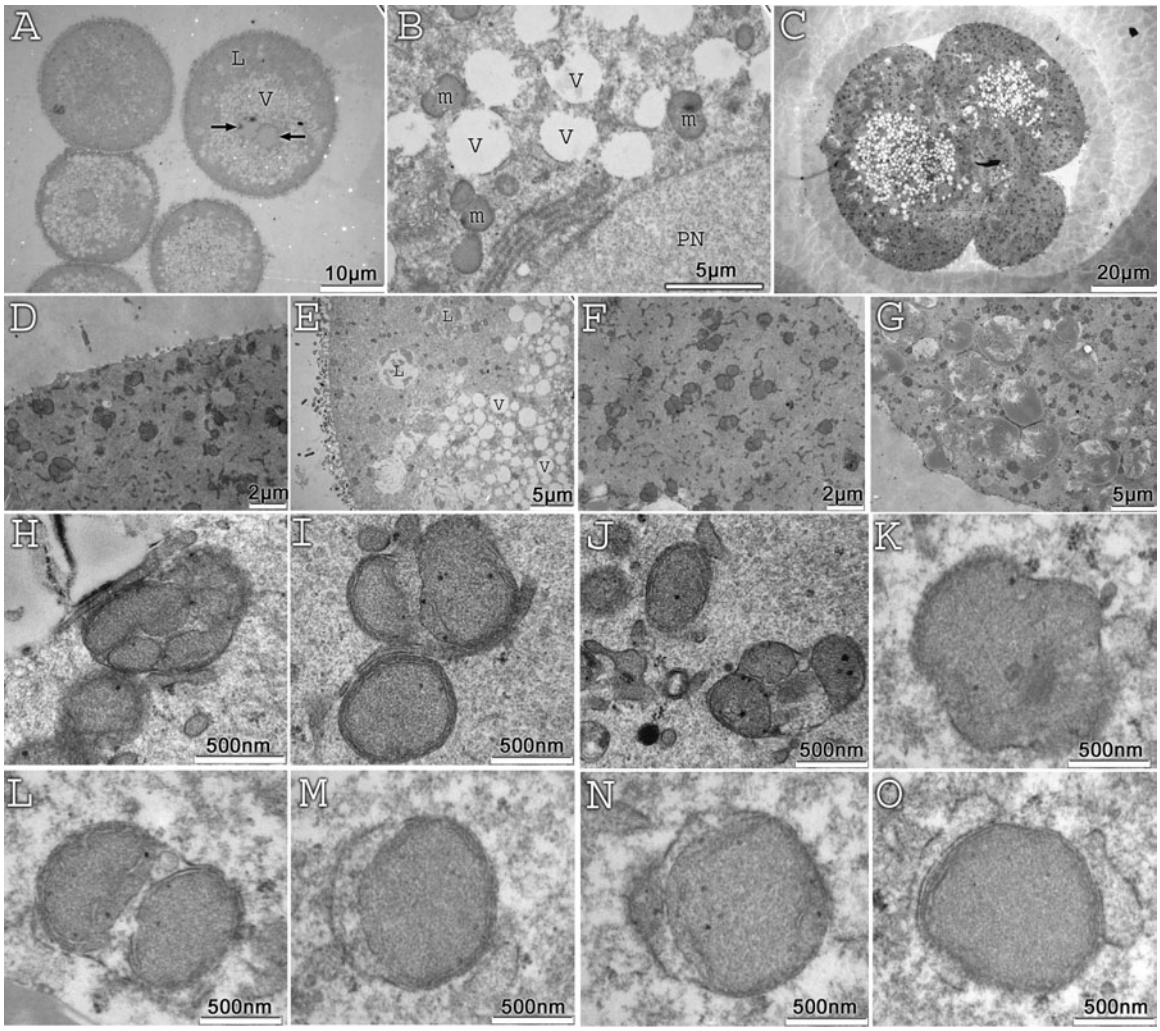

Figure 8. A: TEM of IVF embryos at the pronuclear stage (24 h after insemination). Two pronuclei (arrows) are seen in the cell in the upper right surrounded by electron translucent vesicles (V); lipid droplets (L) are mainly seen toward the cell periphery surrounding the area containing the translucent vesicles. Mitochondria are dispersed within the ooplasm. **B:** Higher magnification showing one of the pronuclei (PN) surrounded by mitochondria (m) and vesicles (V). **C:** 2-cell stage embryo at 48 h after IVF. The smaller third cell is a polar body cell. **D–G**: Mitochondria are dispersed throughout the cytoplasm (48 h after IVF). **H–O:** Various mitochondrial shapes and forms can be distinguished ranging from single to more complex mitochondrial aggregates. Most mitochondria are seen in close association with endoplasmic reticulum, which is either tightly surrounding mitochondria (**I**), in loose association (**J**), or in a network organization that appears to connect the individual mitochondrial aggregates (**I**). Endoplasmic reticulum associated with mitochondria can either be smooth (**M**) or rough (**O**). The more complex shapes and configurations of mitochondrial aggregates are pleomorphic mitochondria. Note the regular dense matrix and absence of mitochondrial cristae as typical for the majority of mitochondria at this stage of development. The dense osmiophilic granules inside mitochondria are matrix granules. In **I** and **J** individual mitochondria are seen as well as small mitochondrial aggregates that typically consist of two or more mitochondrial components. **K–O** shows detail of mitochondria-ER associations. In **H** a pleomorphic mitochondrion is seen in close contact with a lipid droplet.

mitochondria with regular cristae (arrows) surrounding the nucleus in a perinuclear organization pattern.

Porcine IVF Embryos

A three-dimensional (3D) analysis of mitochondria in *in vivo*–fertilized porcine oocytes had been conducted previously (Krause et al., 1992). The present studies are focused on *in vitro* and SCNT pig embryos. The images in Figure 8 present data on IVF oocytes at 24 and 48 h after insemination. In Figure 8A several IVF eggs are shown from the 24-h IVF time point with one egg sectioned in a plane that displays two pronuclei (arrows) surrounded by electron translucent vesicles (V) while lipid droplets (L) are mainly

seen toward the cell periphery surrounding the area containing the translucent vesicles. Mitochondria are dispersed within the ooplasm. Figure 8B shows a higher magnification with one of the pronuclei (PN) surrounded by mitochondria (m) and vesicles (V). Figure 8C displays an egg at the 2-cell stage from the 48-h time point after insemination. The smaller third cell in Figure 8C is a polar body. At this time, mitochondria are dispersed throughout the cytoplasm (Fig. 8D–G) after translocation from the egg cortex where they are located before fertilization. Various mitochondrial shapes and forms can be distinguished ranging from single to more complex mitochondrial aggregates (Fig. 8H–O). Most mitochondria are seen in close association with endoplasmic reticulum, which is either tightly surrounding mitochondria (Fig. 8I) in loose association (Fig. 8J) or in a network organization that appears to connect the individual mitochondrial aggregates (Fig. 8I). Endoplasmic reticulum associated with mitochondria can either be smooth (Fig. 8M) or rough (Fig. 8O). The more complex shapes and configurations of mitochondrial aggregates have been described as pleomorphic mitochondria. Detailed biochemical analysis of these mitochondria and their association with ER membranes has not yet been performed. A regular dense matrix and absence of mitochondrial cristae are typical for the majority of mitochondria at this stage of development. The dense osmiophilic granules inside mitochondria are matrix granules that are thought to be composed of phospholipids, glycolipids, and calcium among other constituents. In Figure 8I,J individual mitochondria are seen as well as small mitochondrial aggregates that typically consist of two or more mitochondrial components. Figure 8K–O has been chosen to show detail of mitochondria-ER associations. In Figure 8H, a pleomorphic mitochondrion is seen in close contact with a lipid droplet.

Porcine NT Embryos

Nuclear transfer of a somatic cell into an enucleated oocyte introduces a donor cell mitochondrial population that along with the enucleated oocyte's mitochondria results in heterogeneous mitochondrial mixing. Figure 9A shows a somatic fetal fibroblast cell at 30 min after fusion within the enucleated oocyte. A large nucleus is seen (N) containing two reticular nucleoli as is typical for somatic cells. The fetal fibroblast cell is still delineated as a separate cell that is more clearly discernible in the higher magnification image in Figure 9B in which somatic cell mitochondria are also seen. The arrows delineate the somatic cell. Large lipid droplets (L) and numerous electron-lucent vesicles of varying sizes are seen in the ooplasm. Figure 9C shows a higher magnification image of the fetal fibroblast cell's mitochondria with well-displayed cristae while typical oocyte mitochondria are round to oval or assembled into more complex mitochondrial aggregations as seen in Figure 9D–K. The egg's mitochondria are mainly distributed along the egg cortex (Fig. 9D) and subsequently distribute toward the egg center as seen in Figure 9E–G at the 30-min time point, in Figure 9H,I at the 6-h time point, and in Figure 9J,K at the 20-h time point. Individual as well as pleomorphic mitochondrial aggregates are seen in all stages of development that have been analyzed in this study.

An NT egg at 20 h after nuclear transfer is shown in Figure 9L. At this time point, the fetal fibroblast cell has incorporated well into the enucleated oocyte, and the nucleus has moved toward the oocyte's cell center (arrow). The two condensed nucleoli within the nucleus indicate that nuclear remodeling has taken place, as dense nucleoli are typical for embryonic cells at this stage of development. Lipid droplets of various sizes and smaller vesicles are seen within the reconstructed embryo cell. Higher magnifications are shown in Figure 9M–P with mitochondria (m), electron translucent vesicles (Fig. 9M,N), various other vesicles and enlarged tubular ER and mitochondria (Fig. 9P) surrounding the nucleus. The aggregated mitochondrial complexes appear to be more frequently localized at the oocyte's periphery while smaller individual mitochondria are seen more frequently around the nucleus in a perinuclear organization pattern.

Details of ultrastructural features in mitochondria from SCNT eggs of the 1-, 6-, and 20-h time points are shown in the higher magnification images displayed in Figure 10. No significant changes in mitochondrial ultrastructure are seen within this time frame, but morphologies within individual oocytes vary greatly. No significant differences are noted between the general ultrastructure of oocyte mitochondria in IVF and SCNT oocytes. The images shown in Figure 10 are representative of all stages, and typical mitochondrial morphologies from SCNT embryos are shown in Figure 10A–J. Figure 10A,B displays mitochondria clusters (1-h NT time point). These clusters display various substructures and appear to be fragmented mitochondrial aggregations surrounding a fibrillar matrix of unknown nature. Figure 10C–G is of the 6-h time point and seen here are clusters with complex substructures of lighter and darker osmiophilic areas as well as complex associations with ER. These mitochondrial clusters are either localized within the ooplasm or close to lipid droplets as seen in Figure 10F,G. In Figure 10D,E long tubular or circular ER is shown in association with mitochondria. Figure 10H–K is of the 20-h NT time point and shows single (Fig. 10H), double (Fig. 10M,P), or multiplexed pleomorphic (10K) forms of mitochondria.

Discussion

Cloning of pigs by SCNT has become an important new area in biomedical research because of the physiological similarity of pigs with humans and the high potential to utilize genetically modified pigs for biomedical applications and as model for human disease (Prather et al., 2003; reviewed in Prather, 2007). However, cloning efficiency is

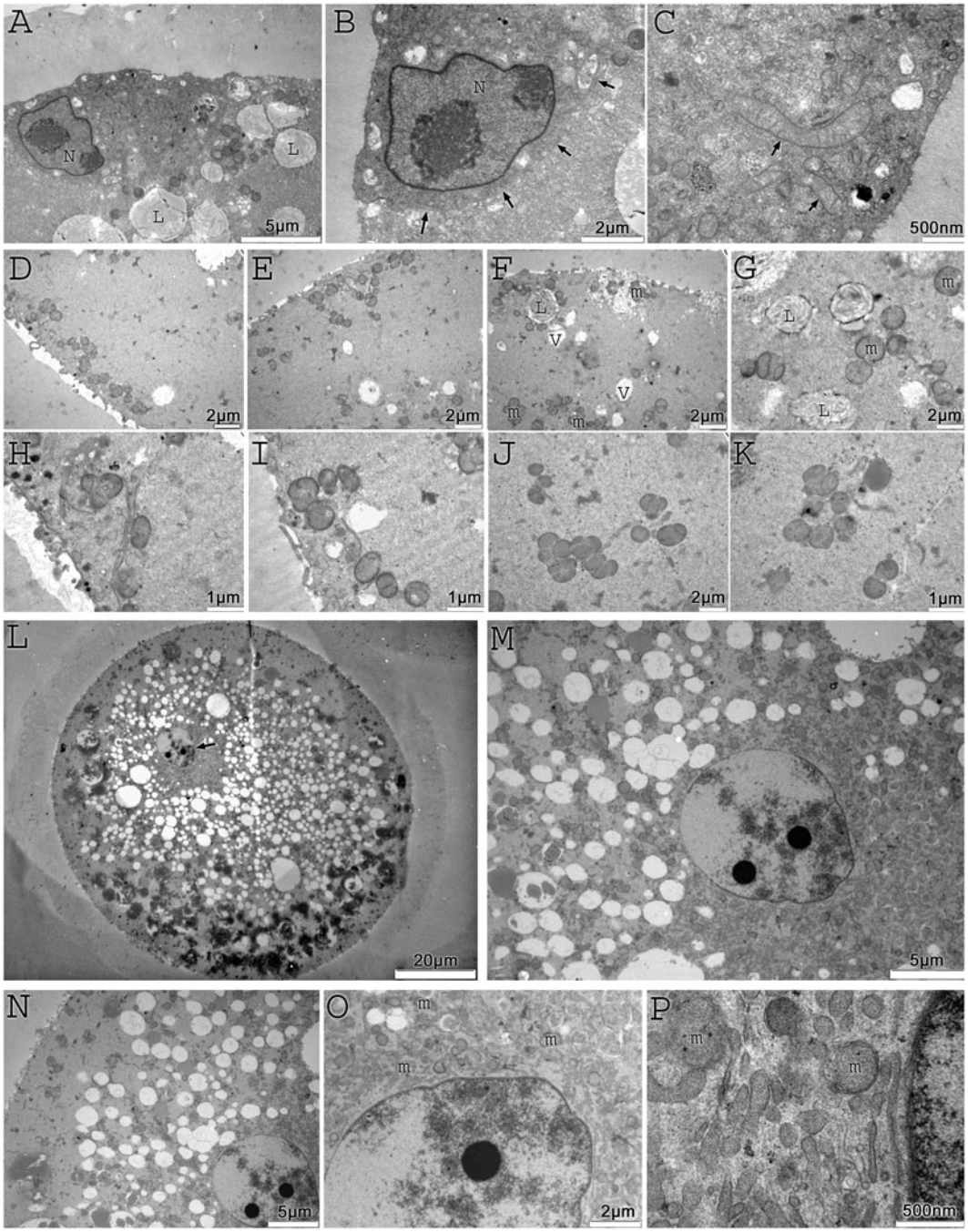

Figure 9. A: TEM of reconstructed oocyte at 30 min after fusion. The donor cell is still clearly separated from the oocyte cytoplasm, and typical somatic cell mitochondria are seen within the donor cell surrounding the donor cell nucleus (N) while the oocyte displays typical embryonic mitochondria. The donor cell nucleus contains reticular nucleoli. Large lipid droplets (L) are seen in the oocyte cytoplasm. **B:** TEM of enlarged area of Figure **9A** showing the areas of donor cell and oocyte interactions (arrows). **C:** Higher magnification TEM image of somatic donor cell mitochondrial morphology with clear cristae (arrows) at 30 min after reconstruction. **D–K:** Typical oocyte mitochondrial configurations displaying round to oval or more complex mitochondrial assemblies. **D:** The egg's mitochondria are mainly distributed along the egg cortex and subsequently distribute toward the egg center (**E–G**) at the 30-min time point. **H**, **I**: 6-h time point. **J–K**: 20-h time point. **L:** A reconstructed egg at 20 h after SCNT. The fetal fibroblast cell has incorporated well into the enucleated oocyte, and the nucleus has moved toward the oocyte's cell center (arrow). The two condensed nucleoli are typical for embryonic cells at this stage of development. Lipid droplets of various sizes and smaller vesicles are seen within the reconstructed embryo cell. **M–P:** Higher magnification images displaying mitochondria (m), electron translucent vesicles (**M**,**N**), various other vesicles and enlarged tubular ER and mitochondria (**P**) around the nucleus.

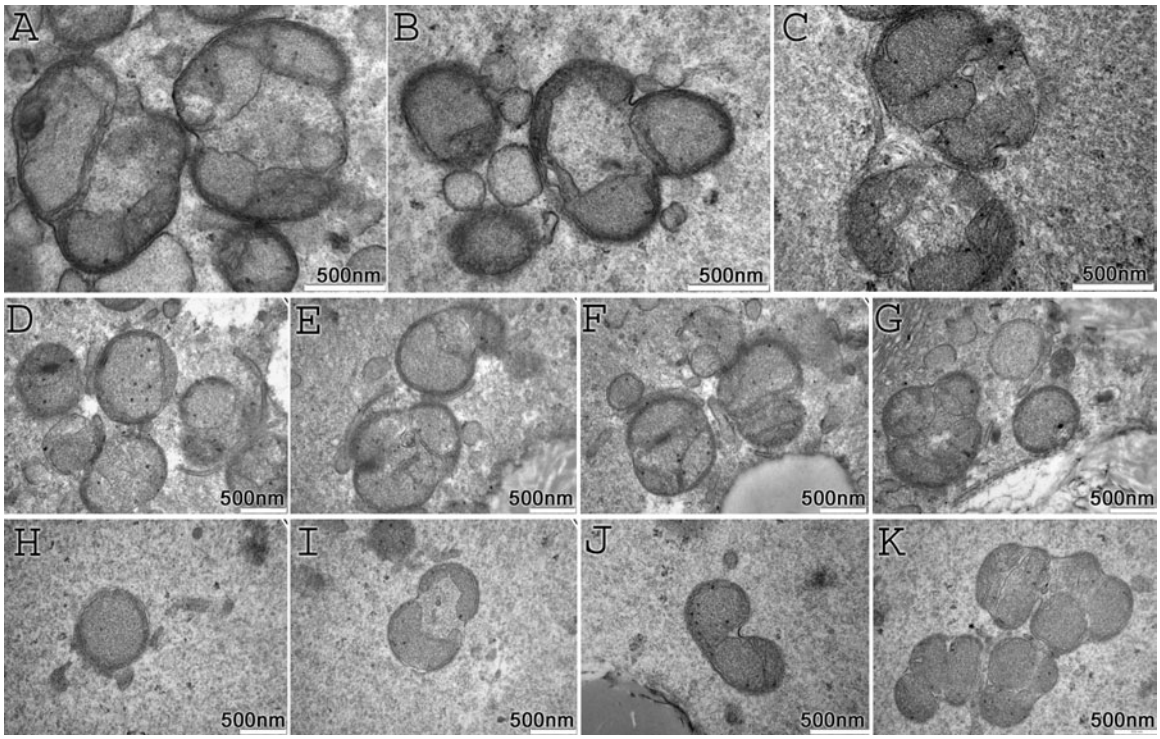

Figure 10. TEM depicting details of ultrastructural features in mitochondria from SCNT eggs from 1-, 6-, and 20-h time points. **A**,**B:** Mitochondrial clusters (1-h NT time point). The clusters display various substructures and appear to be fragmented mitochondrial aggregations surrounding a fibrillar matrix of unknown nature. **C–G:** Clusters with complex substructures of lighter and darker osmiophilic areas as well as complex associations with ER (6-h time point). These mitochondrial clusters are either localized within the ooplasm or close to lipid droplets as seen in **L. D**,**E:** Long tubular or circular ER is seen in association with mitochondria. **H–K:** Single (**H**), double (**I**,**J**), or multiplexed pleomorphic (**K**) forms of mitochondria (20-h NT time point).

still low (ca. 1–2%) and reconstructed embryos frequently display developmental abnormalities in various stages of embryogenesis. Several lines of investigations are underway aimed at improving remodeling of the donor cell nucleus as well as cytoplasmic regulations. Recently, mitochondria have gained particular attention, as translocation of mitochondria from the oocyte cortex to the perinuclear area is significantly lower in SCNT embryos compared to IVF embryos, which has been shown to decrease developmental potential (reviewed in Schatten et al., 2005; Katayama et al., 2006). To address the possible causes for the insufficient mitochondrial translocations, we have performed fluorescence and immunofluorescence microscopy (Katayama et al., 2006) and revealed that sperm factors as well as factors in the meiotic spindle improved developmental potential. The present article expands on these studies to determine whether mitochondrial ultrastructure may also play a role in decreased translocation of mitochondria in SCNT embryos compared to IVF embryos. We also analyzed distribution and fate of donor cell mitochondria. Mitochondrial distribution in cloned pig embryos has not yet been studied on ultrastructural levels, and kinetics of donor cell mitochondrial distribution is also a new field of investigation.

Oocyte mitochondria display totally different ultrastructures compared to somatic cell mitochondria. Several different morphologies are seen on ultrastructural levels, perhaps indicating that different mitochondria may carry out different functions. The ultrastructure of various mammalian oocytes has been described (Senger & Saacke, 1970; Szöllösi, 1972; Calarco & McLaren, 1976; Cran, 1985; Krause et al., 1992; Ullmann & Butcher, 1996; and references cited therein), and various mitochondrial morphologies have been identified including single round-oval, dumbbell-shaped, hooded, pleomorphic, and vacuolated mitochondrial morphologies. Mitochondrial morphologies vary to some extent in different mammalian species. Hooded mitochondria morphologies are more frequent in bovine embryos while fenestrated mitochondria have been reported for marsupials as well as bovine and pig embryos (Krause et al., 1992; Ullmann & Butcher, 1996; present report), but the significance for these morphological specifications is not known. Vacuole formation had been reported for marsupials to be the result of mitochondrial restructuring (Ullmann & Butcher, 1996), but no such vacuolization has been reported for pig oocytes, including the present report. Most of the described oocyte mitochondria contain an osmiophilic matrix of fibril-

lar material and matrix granules that are thought to be composed of phospholipids, glycolipids, and calcium among other constituents. The absence of cristae and inclusion of osmiophilic matrix and fibrillar material is characteristic for most oocyte mitochondria. Building on previous studies by Cran (1985), Krause et al. (1992) produced a 3D reconstruction of pleomorphic mitochondrial aggregates for porcine oocytes, zygotes, and early embryos and determined that the mitochondrial aggregates primarily consist of two to three interconnected mitochondria surrounding an area of cytoplasmic matrix composed of amorphous and fibrillar material of yet to be determined nature, although it has been proposed that the matrix may contain hormones or enzymes that are needed for development of the early embryo (discussed in Krause et al., 1992). Each of the aggregates was shown to be enveloped by smooth endoplasmic reticulum.

The present study is the first, to our knowledge, to analyze mitochondria on ultrastructural levels in IVF and SCNT pig oocytes. Our results in IVF and SCNT embryos generally agree with the earlier report on mitochondria observed in *in vivo*–produced embryos, but we also noted several morphologies with highly complex structural features. In addition, some of these complex multimitochondrial aggregates appeared to be in a state of disaggregation, perhaps mixing some contents with the oocyte's cytoplasm. In general, we did not find significant differences between mitochondria of IVF and SCNT oocytes. However, we noted fewer pleomorphic mitochondria around the SCNT nucleus while the single round-oval smaller mitochondria population was more frequently accumulated in the perinuclear area. It is possible that a subgroup of the entire mitochondrial population in SCNT eggs is translocated preferentially to the perinuclear area compared to the mitochondrial population in *in vivo*– and *in vitro*–fertilized embryos. Further studies are needed to quantitate the distribution of morphologically different mitochondria and ascribe functions to the different and complex structural variations. Such studies are complex and have not yet been attempted. At the present time, it is not clear whether different mitochondrial morphologies within single oocytes and embryos indicate varied functions and different activities that may be different in SCNT compared to IVF pig embryos. Compared to somatic cell mitochondria, very little is known about mitochondrial functions in preimplantation embryos, as structure-function relationships have not yet been explored.

Dynamic translocations of mitochondria are critically important for temporal-spatial metabolic activities that allow embryo development and survival. In a number of mammalian species, including the pig, mitochondrial translocation from the egg cortex to the ooplasm and to the perinuclear area has been correlated with positive developmental potential (Sun et al., 2001; reviewed in Schatten et al., 2005; Katayama et al., 2006). Functional microtubules are critically important for mitochondria translocation from the oocyte cortex to the perinuclear area (Katayama et al., 2006). However, microtubule organization is different in IVF eggs compared to SCNT eggs. In SCNT eggs, microtubules are organized from the donor cell centrosome. In IVF eggs, microtubules are organized by the sperm centrosome that results in sperm aster formation after fertilization. It is possible that microtubules organized by the donor cell centrosome are not fully able to translocate oocyte mitochondria.

Other complexities resulting from SCNT are caused by the heterogeneous mitochondrial population that consists of oocyte mitochondria as well as donor cell mitochondria. In IVF eggs, sperm mitochondria are incorporated into the ooplasm but become degraded by oocyte-driven ubiquitination (Sutovsky et al., 1999, 2003; Sutovsky, 2004) resulting in the homogeneous mitochondrial population that is characteristic for *in vitro*– and *in vivo*–fertilized embryos. Unlike sperm mitochondria, the donor cell mitochondria are typically not degraded, which has been reported for several mammalian species (Steinborn et al., 2000; reviewed in Schatten et al., 2005), and it has been proposed that donor cell mitochondria in SCNT eggs may exert negative effects on embryo development, but the exact causes and the extent have not yet been investigated. In the present study we utilized our YFP-mitochondria cell line derived from mouse tissue (Zhong et al., 2007) to study donor cell mitochondrial distribution. Interspecies SCNT has been used in numerous previous studies to follow the contribution and influence of donor cell mitochondria to the developing reconstructed embryos, and it has emerged as an important tool to study nucleo-cytoplasmic interactions (Uhm et al., 2007). The inheritance pattern of donor cell mitochondria varies in different species and has become an active area of investigations (Steinborn et al., 2000, 2002; Hiendleder et al., 2004; St. John et al., 2004; Murakami et al., 2005; reviewed in Schatten et al., 2005; Takeda et al., 2006; Ferreira et al., 2007). Transmission of donor cell mitochondrial DNA (mtDNA) has been reported for pigs and progeny (Takeda et al., 2006) while this is not the case for reconstructed bovine embryos (Ferreira et al., 2007). In most species, oocyte mitochondria dominate the entire SCNT embryo mitochondrial population, although it has been reported for panda that donor cell mitochondria dominated in early fetuses after implantation (Chen et al., 2002). In the present study we used the interspecies SCNT approach coupled with YFP-mitochondria tracking of 3T3 cells to clearly distinguish donor cell mitochondria from the recipient oocyte mitochondria. We found that donor cell mitochondria are introduced along with the donor cell nucleus and initially remain closely associated with the donor cell nucleus but then distribute either evenly or unevenly into the dividing blastomere cells, which was observed for both intra- or interspecies SCNT embryos. The importance of equal mitochondrial distribution has been addressed in various studies (Van Blerkom et al., 1995, 2000; Squirrell et al., 1999, 2001, 2003; Sun et al., 2001), and it has been shown that disproportional patterns of mitochondrial inheritance in 2–4-cell human embryos results in cell lysis of the blastomere that is

deficient in mitochondria (Van Blerkom et al., 2000). We found equal mitochondrial distribution to the two blastomeres in 82.8% and unequal distribution that was observed in 17.2%, raising the possibility that unequal distribution may exert negative effects and play a role in developmental problems. In IVF human oocytes (Van Blerkom et al., 2000), unequal mitochondrial distribution resulted in lysis of blastomeres creating an imbalance in total cell numbers during development. In SCNT embryos, it is possible that an accumulation of donor cell mitochondria in one blastomere might communicate signals to the oocyte's mitochondrial population to undergo apoptosis. Increased apoptosis in the developing embryo is indeed seen more frequently in SCNT embryos (Hao et al., 2003). Long-term studies are needed to clarify whether somatic cell mitochondria exert a negative effect on development of the reconstructed embryo.

In the present study we showed that oocyte and somatic cell mitochondria were initially segregated but mixed within 8 h after SCNT. Morphological differences between donor cell and oocyte mitochondria may play a role in incomplete mitochondrial translocations in NT pig embryos. It is possible that mitochondria with different morphologies are translocated differently, and it is also possible that some oocyte mitochondrial morphologies or mitochondrial surface structures may be incompatible for translocation along microtubules that are organized by donor cell centrosomes (Zhong et al., 2007) compared to those organized by the sperm centrosomes as is the case in *in vivo*– and *in vitro*–fertilized oocytes. The surfaces of oocyte mitochondria appear to be complex in that they are frequently associated with endoplasmic reticulum or other lamellar structures that may prevent association with microtubules generated by donor cell centrosomes. Further investigations are needed to analyze on molecular levels potential compatibility issues related to components and molecular motors that associate with mitochondrial membranes and whether differences exist regarding mitochondrial translocation along donor cell–generated microtubules compared to sperm aster microtubules. Abnormalities in translocation may be a problem in SCNT embryos; it has been reported that abnormal mitochondrial structure in human oocytes resulted in incomplete mitochondrial translocations and arrested development (Au et al., 2005).

Taken together, our results have shown that donor cell mitochondria incorporate into the reconstructed embryo's mitochondrial pool and can be visualized up to day 6 of development. We showed that mitochondrial cristae as typical for somatic cells are characteristically missing in oocyte cells. Instead, a large matrix fills most of the mitochondrial space. Little is known about the surface structure of oocyte mitochondria, and the possibility exists that oocyte mitochondria and microtubules nucleated by the somatic cell centrosome in SCNT reconstructed embryos may not be entirely compatible for translocation to the perinuclear area, which could play a role in the incomplete mitochondrial distribution to the perinuclear area in SCNT embryos.

Acknowledgments

This work was supported by the National Institutes of Health (R03-HD047309-01 to H.S. and R01-RR013438-08 to R.S.P.)

References

Abeydeera, L.R., Wang, W.H., Prather, R.S. & Day, B.N. (1998). Maturation *in vitro* of pig oocytes in protein-free culture media: Fertilization and subsequent embryo development *in vitro*. *Biol Reprod* **58**, 1316–1320.

Au, H.-K., Yeh, T.-S., Kao, S.-H., Tzeng, C.-R. & Hsieh, R.-H. (2005). Abnormal mitochondrial structure in human unfertilized oocytes and arrested embryos. *Ann NY Acad Sci* **1042**, 177–185.

Calarco, P.G. (1995). Polarization of mitochondria in the unfertilized mouse oocytes. *Dev Genet* **16**, 36–46.

Calarco, P.G. & McLaren, A. (1976). Ultrastructural observations of preimplantation stages of the sheep. *J Embryol Exp Morph* **36**, 609–622.

Chen, D-Y., Wen, D-C., Zhang, Y-P., Sun, Q-Y., Han, Z-M., Liu, Z-H., Shi, P., Li, J-S., Xiangyu, J-G., Lian, L., Kou, Z-H., Wu, Y-Q., Chen, Y-C., Wang, P-Y. & Zhang, H-M. (2002). Interspecies implantation and mitochondria fate of panda-rabbit cloned embryos. *Biol Repro* **67**, 637–642.

Cran, D.G. (1985). Qualitative and quantitative structural changes during pig oocyte maturation. *J Reprod Fertil* (Suppl) **38**, 49–62.

Ferreira, C.R., Meirelles, F.V., Yamazaki, W., Chiaratti, M.R., Méo, S.C., Perecin, F., Smith, L.C. & Garcia, J.M. (2007). The kinetics of donor cell mtDNA in embryonic and somatic donor cell-derived bovine embryos. *Cloning Stem Cells* **9**(4), 618–629.

Han, Y.-M., Abeydeera, L.R., Kim, J.-H., Moon, H.-B., Cabot, R.A., Day, B.N. & Prather, R.S. (1999*a*). Growth retardation of inner cell mass cells in polyspermic porcine embryos produced *in vitro*. *Biol Reprod* **60**, 1110–1113.

Han, Y.M., Wang, W.H., Abeydeera, L.R., Petersen, A.L., Kim, J.H., Murphy, C., Day, B.N. & Prather, R.S. (1999*b*). Pronuclear localization before the first cell division determines ploidy of polyspermic pig embryos. *Biol Reprod* **61**, 1340–1346.

Hao, Y., Lai, L., Mao, J., Im, G.-S., Bonk, A. & Prather, R. (2003). Apoptosis and *in vitro* development of preimplantation porcine embryos derived *in vitro* or by nuclear transfer. *Biol Reprod* **69**, 501–507.

Hiendleder, S., Prelle, K., Brüggerhoff, K., Reichenack, H.-D., Wenigerkind, H., Bebbere, D., Stojkoviv, M., Müller, S., Brem, G., Zakhartchenko, V. & Wolf, E. (2004). Nuclear-cytoplasmic interactions affect *in utero* developmental capacity, phenotype, and cellular metabolism of bovine nuclear transfer fetuses. *Biol Reprod* **70**, 1196–1205.

Katayama, M., Zhong, Z.-S., Lai, L., Sutovsky, P., Prather, R.S. & Schatten, H. (2006). Mitochondria distribution and microtubule organization in fertilized and cloned porcine embryos: Implications for developmental potential. *Dev Biol* **299**, 206–220.

Krause, W.J., Charlson, E.J., Sherman, D.M. & Day, B.N. (1992). Three-dimensional reconstruction using a computer graphics system: Application to mitochondrial aggregates in porcine

oocytes, zygotes, and early embryos using a personal computer. *Zool Anz* **229**, 21–36.

Lai, L., Park, K.W., Cheong, H.T., Kühholzer, B., Samuel, M., Bonk, A., Im, G.S., Rieke, A., Day, B.N., Murphy, C.N., Carter, D.B. & Prather, R.S. (2002). Transgenic pig expressing the enhanced green fluorescent protein produced by nuclear transfer using colchicine-treated fibroblasts as donor cells. *Mol Reprod Dev* **62**(3), 300–306.

Li, R., Lai, L., Wax, D., Hao, Y., Murphy, C.N., Rieke, A., Samuel, M., Linville, M.L., Korte, S.W., Evans, R.W., Turk, J.R., Kang, J.X., Witt, W.T., Dai, Y. & Prather, R.S. (2006). Cloned transgenic swine via *in vitro* production and cryopreservation. *Biol Reprod* **75**, 226–230.

Murakami, M., Otoi, T., Wongsrikeao, P., Agung, B., Sambuu, R. & Suzuki, T. (2005). Development of interspecies cloned embryos in yak and dog. *Cloning Stem Cells* **7**(2), 77–81.

Petters, R.M. & Wells, K.D. (1993). Culture of pig embryos. *J Reprod Fertil Suppl* **48**, 61–73.

Prather, R.S. (2007). Nuclear remodeling and nuclear reprogramming for making transgenic pigs by nuclear transfer. In *Somatic Cell Nuclear Transfer*, Sutovsky, P. (Ed.), Landes Bioscience. *Adv Exp Med Biol* **591**, 1–13.

Prather, R.S., Hawley, R.J., Carter, D.B., Lai, L. & Greenstein, J.L. (2003). Transgenic swine for biomedicine and agriculture. *Theriogenol* **59**, 115–123.

Schatten, H., Prather, R.S. & Sun, Q.-Y. (2005). The significance of mitochondria for embryo development in cloned farm animals. *Mitochondrion* **5**, 303–321.

Schatten, H., Ripple, M., Balczon, R., Weindruch, R. & Taylor, M. (2000*a*). Androgen and taxol cause cell type specific alterations of centrosome and DNA organization in androgen-responsive LNCaP and androgen-independent prostate cancer cells. *J Cell Biochem* **76**, 463–477.

Schatten, H. & Ris, H. (2002). Unconventional specimen preparation techniques using high resolution low voltage field emission scanning electron microscopy to study cell motility, host cell invasion, and internal structures in *Toxoplasma gondii*. *Microsc Microanal* **8**, 94–103.

Schatten, H. & Ris, H. (2004). Three-dimensional imaging of *Toxoplasma gondii*—Host cell membrane interactions. *Microsc Microanal* **10**, 580–585.

Schatten, H., Wiedemeier, A., Taylor, M., Lubahn, D., Greenberg, M.N., Besch-Williford, C., Rosenfeld, C., Day, K. & Ripple, M. (2000*b*). Centrosome-centriole abnormalities are markers for abnormal cell divisions and cancer in the transgenic adenocarcinoma mouse prostate (TRAMP) model. *Biol Cell* **92**, 331–340.

Senger, P.L. & Saacke, R.G. (1970). Unusual mitochondria of the bovine oocyte. *J Cell Biol* **46**, 405–408.

Squirrell, J.M., Lane, M. & Bavister, B.D. (2001). Altering intracellular pH disrupts development and cellular organization in preimplantation hamster embryos. *Biol Reprod* **64**, 1845–1854.

Squirrell, J.M., Schramm, R.D., Paprocki, M., Wokosin, D.L. & Bavister, B.D. (2003). Imaging mitochondrial organization in living primate oocytes and embryos using multiphoton microscopy. *Microsc Microanal* **9**, 190–201.

Squirrell, J.M., Wokosin, D.L., Bavister, B.D. & White, J.G. (1999). Long-term multiphoton fluorescence imaging of mammalian embryos does not compromise viability. *Nature Biotechn* **17**, 763–767.

Steinborn, R., Schinogl, P., Wells, D.N., Bergthaler, A., Müller, M. & Brem, G. (2002). Coexistence of *Bos taurus* and *B. indicus* mitochondrial DNA in nuclear transfer-derived somatic cattle clones. *Genetics* **162**, 823–829.

Steinborn, R., Schinogl, P., Zakhartchenko, V., Achmann, R., Schernthaner, W., Stojkovic, M., Wolf, E., Müller, M. & Brem, G. (2000). Mitochondrial DNA heteroplasmy in cloned cattle produced by fetal and adult cell cloning. *Nature Gen* **25**, 255–257.

St. John, J.C., Lloyd, R.E.I., Bowles, E.J., Thomas, E.C. & Shourbagy, S.E. (2004). The consequences of nuclear transfer for mammalian foetal development and offspring survival. A mitochondrial DNA perspective. *Reproduction* **127**, 631–641.

Sun, Q.-Y, Wu, G.M., Lai, L., Park, K.W., Day, B., Prather, R.S. & Schatten, H. (2001). Translocation of active mitochondria during porcine oocyte maturation, fertilization and early embryo development *in vitro*. *Reproduc* **122**, 155–163.

Sutovsky, P. (2004). Degradation of paternal mitochondria after fertilization: Implications for heteroplasmy, assisted reproductive technologies and mtDNA inheritance. *Reprod Bio Med* **8**, 24–33.

Sutovsky, P., McCauley, T.C., Sutovsky, M. & Day, B.N. (2003). Early degradation of paternal mitochondria in domestic pig (Sus scrofa) is prevented by selective proteasomal inhibitors lactacystin and MG 132. *Biol Reprod* **68**, 1793–1800.

Sutovsky, P., Moreno, R.D., Ramalho-Santos, J., Dominko, T., Simerly, C. & Schatten, G. (1999). Ubiquitin tag for sperm mitochondria. *Nature* **402**, 371–372.

Szöllösi, D. (1972). Changes of some cell organelles during oogenesis in mammals. In *Oogenesis*, Biggars, J.D. & Schuetz, A.W. (Ed.), pp. 47–64. Baltimore, MD: University Press.

Takeda, K., Tasai, M., Iwamoto, M., Akita, T., Tagami, T., Nirasawa, K., Hanada, H. & Onishi, A. (2006). Transmission of mitochondrial DNA in pigs and progeny derived from nuclear transfer of Meishan pig fibroblast cells. *Mol Repro Dev* **73**, 306–312.

Uhm, S.J., Gupta, M.K., Kim, T. & Lee, H.T. (2007). Expression of enhanced green fluorescent protein in porcine- and bovine-cloned embryos following interspecies somatic cell nuclear transfer of fibroblasts transfected by retrovirus vector. *Mol Repro Dev* **74**, 1538–1547.

Ullmann, S.L. & Butcher, L. (1996). Mammalian oocyte organelles with special reference to pleomorphic mitochondria and vacuole formation in marsupials. *Reprod Fertil Dev* **8**, 491–508.

Van Blerkom, J., Davis, P. & Alexander, S. (2000). Differential mitochondrial distribution in human pronuclear embryos leads to disproportionate inheritance between blastomeres: Relationship to microtubular organization, ATP content and competence. *Human Reproduction* **15**, 2621–2633.

Van Blerkom, J., Davis, P. & Lee, J. (1995). ATP content of human oocytes and developmental potential and outcome after *in vitro* fertilization and embryo transfer. *Human Reproduction* **10**, 415–424.

Zhong, Z., Spate, L., Hao, Y., Li, R., Lai, L., Katayama, M., Sun, Q.Y., Prather, R.S. & Schatten, H. (2007). Remodeling of centrosomes in intraspecies and interspecies nuclear transfer porcine embryos. *Cell Cycle* **6**(12), 1510–1521.

Zhong, Z.-S., Zhang, G., Meng, X.-Q., Zhang, Y.-L., Chen, D.-Y., Schatten, H. & Sun, Q.-Y. (2005). Function of donor cell centrosome in intraspecies and interspecies nuclear transfer embryos. *Exp Cell Res* **306**, 35–46.